COMPDYN 2015
5th ECCOMAS Thematic Conference on
Computational Methods in Structural Dynamics and Earthquake Engineering
M. Papadrakakis, V. Papadopoulos, V. Plevris (eds.)
Crete Island, Greece, 25–27 May 2015

IN PLAN DISTRIBUTION OF ISOLATORS EFFECTIVE STIFFNESS FOR MINIMIZING THE TORSIONAL RESPONSE OF BASE ISOLATED BUILDINGS

K. Kostinakis[1], A. Athanatopoulou[2], D. Arampatzi[3] and A. Atsalos[4]

[1] Post-Doctoral Researcher, Department of Civil Engineering, Aristotle University of Thessaloniki
Aristotle University campus, 54124, Thessaloniki, Greece
e-mail: kkostina@civil.auth.gr

[2] Professor, Department of Civil Engineering, Aristotle University of Thessaloniki
Aristotle University campus, 54124, Thessaloniki, Greece
e-mail: minak@civil.auth.gr

[3,4] Civil Engineer, Department of Civil Engineering, Aristotle University of Thessaloniki
Aristotle University campus, 54124, Thessaloniki, Greece

Keywords: Base Isolation, Torsional Response, R/C Buildings, Effective Stiffness of Isolators, Time History Analysis.

Abstract. *The present study examines the influence of the isolators' effective stiffness distribution on the torsional response of base isolated structures. To accomplish this purpose two asymmetric in plan R/C buildings are analyzed for two different distributions of isolators' effective stiffness: (a) all the isolators have identical horizontal stiffness and (b) the isolators' effective stiffness is chosen so as the optimum torsion axis of the structure to coincide with the vertical mass axis. The two buildings are subjected to linear as well as nonlinear time history analyses under three bidirectional earthquake ground motions. For each earthquake record the maximum response over all incident angles of seismic motion is determined. The analyses results reveal that the displacements of the structural elements located at the flexible side of the buildings as well as the rotations of the slabs are reduced significantly when the isolators' effective stiffness is chosen so as the optimum torsion axis of the structure to coincide with the vertical mass axis.*

1 INTRODUCTION

Base isolation has been used as one of the most wildly accepted seismic protection system. It consists of a flexible material which is provided at the base of the building in order to reduce the seismic forces induced to the structure. The isolators, which are installed between the ground and the upper structure, are designed to decrease the seismic forces applied to the building under strong ground motions and as a consequence to reduce damage to the primary structural members. In addition base isolation minimizes damage to secondary members as well as to equipment inside the building. The isolators' flexibility increases the vibration period of the total structure and, as a consequence, the seismic forces induced to the building are reduced. Isolators' flexibility also leads to increase of the horizontal displacements. However, it's possible to control them through increase of damping.

Crosbie [1] first reasoned that by designing the centre of yield forces of the base isolation system (CYF) to coincide with the mass centre of the superstructure (CM) results in significant reduction in the post-yield response of asymmetric structures. Lee [2] suggested that the rigidity centre of the base isolation system (CRB) should be designed to coincide with the CM. The above mentioned researchers reached to the conclusion that this design practically eliminates the effects of asymmetry in the elastic range. Moreover for an equal level of yield stresses in all the bearings this is also true in the inelastic range.

Colunga and Cruz [3] studied the seismic codes suggestions concerning the seismic analysis of asymmetric base isolated buildings. They conducted a parametric study in order to evaluate the seismic code provisions regarding the simplified methods of analysis for asymmetric base-isolated buildings. They studied the effects of the following parameters on isolators' response: a) the ratio T_I / T_s (T_I is the effective period of the isolated building at the design displacement and T_s the elastic period of the fixed based building), b) mass eccentricity in the superstructure and c) stiffness eccentricity in the superstructure. With the aid of this study they defined the limits of structural irregularity for base isolated structures regarding the application of linear methods of analysis.

Kilar and Koren [4] conducted a parametric study for three levels of mass asymmetry, three levels of torsional rigidity of the superstructure and six various distributions of bearings in the isolation system. All these variants were applied on a selected realistic RC frame building structure designed according to Eurocodes 2 [5] and 8 [6].They tried to determine the most favourable distribution of isolators that is able to balance the effects of eccentricities in the superstructure. The results obtained by 3D nonlinear dynamic analyses indicate that all six considered distributions of bearings, reduce the unfavourable torsional effects, which are with different extent transferred from the superstructure to the base isolation system. Also it was observed that CI=CM distribution (CI is the center of isolators and CM the mass center of the superstructure), suggested by some building codes does not minimize torsional effects in base isolated buildings.

In a recent study [7] a methodology that leads to optimal torsional control of base isolated buildings is presented. The methodology is based on the assumption that the superstructure acts as a rigid body. The methodology provides a choice of the optimal eccentricity and torsional stiffness parameters of the isolation system that minimize the lateral-torsional response of the superstructure. Results obtained by probabilistic technique show that the response of the superstructure may be substantially improved if the center of stiffness of the isolators lie in the vicinity of the (average) center of stiffness of the superstructure. Therefore in order to minimize torsional effects in base isolated asymmetric structures it is necessary to introduce eccentricity in the isolation system.

From the above mentioned papers it is derived that there is no consensus on the choice of isolators' properties for minimizing torsional effects in base isolated asymmetric buildings. Some codes [8, 9] suggest that the rigidity center of the base isolation system (CRB) should coincide with the mass center (CM). However, as it mentioned above it has not been proved that this coincidence minimizes the torsional response.

In the present study two R/C 3-storey buildings are analyzed under bi-directional earthquake ground motions for the following two distributions of isolators' effective stiffness: (a) all the isolators have identical horizontal stiffness and (b) the isolators' effective stiffness is chosen so as the optimum torsion axis of the structure to coincide with the vertical mass axis. Note that the total horizontal and torsional stiffness of the isolators should remain approximately constant between the cases (a) and (b). Linear and nonlinear time history analyses under three bidirectional earthquake records are performed and the maximum response over all seismic incident angles is determined. The analyses results reveal that the displacements of the structural elements located at the flexible side of the buildings are reduced significantly in case of model (b). However, the displacements of the structural elements located at the stiff side are either smaller or slightly larger. Furthermore, there is a significant reduction of the diaphragm rotations of model (b) compared to the rotations of model (a). As a general conclusion, we can say that distribution (b) minimizes the torsional response of asymmetric buildings.

2 DESCRIPTION OF THE BUILDINGS AND BASE ISOLATORS

2.1 Description and design of the buildings

For the purposes of the present investigation two 3D R/C buildings (Building 1 and Building 2), with data supplied in figure 1, are studied. The buildings have three stories and their structural systems consist of vertical elements in two perpendicular directions (axes x and y). The dimensions of the structural elements' cross section are shown in Tables 1 and 2.

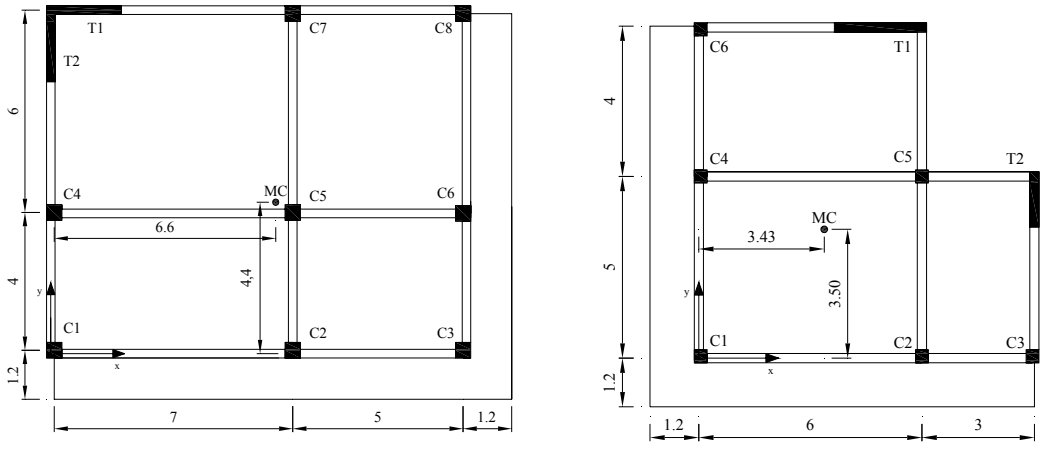

Figure 1. Plan view and geometrical parameters. Building B1 (a) and B2 (b).

For the elastic modeling and design of the buildings, all basic recommendations of EC8 [6] were taken into consideration, such as the diaphragmatic behavior of the slabs, the rigid zones in the joint regions of beams/columns and beams/walls, and the values of flexural and shear stiffness corresponding to cracked R/C elements. The two structures were analyzed using the

modal response spectrum analysis, as described in EC8. The R/C structural elements were designed following the clauses of EC2 [5] and EC8 [6].

	1st Storey	2nd Storey	3rd Storey
Beams (cm)	25/60	25/60	25/60
Columns (cm)	45/45	40/40	30/30
Wall T1 (cm)	25/220	25/220	25/220
Wall T2 (cm)	25/220	25/220	25/220

Table 1: Dimensions of the structural elements' cross sections for building B1.

	1st Storey	2nd Storey	3rd Storey
Beams (cm)	25/60	25/60	25/60
Columns (cm)	35/35	35/35	30/30
Wall T1 (cm)	25/250	25/250	25/250
Wall T2 (cm)	25/150	25/150	25/150

Table 2: Dimensions of the structural elements' cross sections for building B2.

2.2 Isolators' properties

One of the most widely used types of isolators is the Lead Rubber Bearing (LRB), which consists of alternating laminations of thin rubber layers and steel plates, bonded together to provide vertical rigidity and horizontal flexibility. Vertical rigidity assures the isolator will support the weight of the structure, while horizontal flexibility converts destructive horizontal shaking into gentle movement [10]. Moreover, at the centre of laminated natural rubber a lead plug is embedded. Note that the laminated natural rubber demonstrates spring capability, while the lead plug demonstrates damping capability. The seismic response of the isolators depends on their special properties, which are the horizontal effective stiffness, the vertical effective stiffness, as well as the damping. For the two buildings presented in the previous paragraph LRB are used as seismic isolation system. Furthermore, three different models are analyzed:

(a) The buildings are considered as fully fixed to the ground.

(b) All isolators possess the same properties (no eccentricity in the base isolation system exists): The buildings rest on rubber base isolators with vertical effective stiffness k_{veff}=100000 kN/m, horizontal effective stiffness k_{eff}=2000 kN/m and torsional stiffness k_t=5000 kNm/rad. The isolators' damping was taken equal to 30%. Note that the choice of the aforementioned isolators' properties was made bearing in mind that the fundamental period of the base isolated buildings must be approximately three times the fundamental period of the fully fixed to the ground buildings.

(c) Isolators with eccentricity: The buildings rest on base isolators with vertical effective stiffness k_{veff}=100000 kN/m and torsional stiffness k_t=5000 kNm/rad. However, regarding the horizontal effective stiffness, for each building three different types of isolators are available and can be used. For the building B1 the three types of isolators are the following: (i) isolators with k_{eff}=1000 kN/m, (ii) isolators with k_{eff}=1550 kN/m and (iii) isolators with k_{eff}=2950 kN/m. For the building B2 the three available types of isolators are the following: (i) isolators with k_{eff}=1000 kN/m, (ii) isolators with k_{eff}=1400 kN/m and (iii) isolators with k_{eff}=3400 kN/m. The isolators' damping was taken equal to 30% for both the buildings. The distribution of the above three types of isolators in plan was chosen so as the optimum torsion axis (OTA)

of the structures [11, 12] to coincide with the vertical mass axis. Moreover, note that the total horizontal and torsional stiffness of the isolators should remain approximately constant between the cases (b) and (c). For the building B1 the total horizontal and torsional stiffness of the isolators is 20000 kN/m and 893560 kNm/rad for model (b) (772619kNm/rad for model (c)) respectively. For the building B2 the total horizontal and torsional stiffness of the isolators is 16000 kN/m and 469257 kNm/rad for model (b) (462823kNm/rad for model (c)) respectively.

2.3 Determination of the Optimum Torsion Axis

For the two buildings considered the location of the Optimum Torsion Axis (OTA) was determined. Then, the properties of the isolators as well as their in-plan arrangement were determined for case (c) of the previous paragraph. For the determination of the OTA the methodology proposed by Marino and Rossi [11] was used. Then the principal directions under lateral loading were determined using the methodology presented in [12]. According to the aforementioned studies [11, 12] the process of determining the OTA is as follows: Let there be N-storey building system with horizontal rigid floor diaphragms at the floor levels, in a Cartesian global coordinate system Oxyz with a vertical Oz axis (figure 1). Considering as degrees of freedom of the i^{th} floor level the diaphragm rotation θ_{zi} and the horizontal displacements u_{xi} and u_{yi} of a point on the diaphragm, the displacement state of the diaphragms can be characterized by the N-column vectors:

$$\boldsymbol{u}_x = \left[u_{x1}, u_{x2}, \ldots \ldots, u_{xN}\right]^T \tag{1}$$

$$\boldsymbol{u}_y = \left[u_{y1}, u_{y2}, \ldots \ldots, u_{yN}\right]^T \tag{2}$$

$$\boldsymbol{\theta}_z = \left[\theta_{z1}, \theta_{z2}, \ldots \ldots, \theta_{zN}\right]^T \tag{3}$$

Let us also consider the action of a given distribution of horizontal forces:

$$\boldsymbol{F} = \left[F_1, F_2, \ldots \ldots, F_N\right]^T \tag{4}$$

that belong to a vertical loading plane and pass through a vertical loading axis. Note that for the fully fixed to the ground buildings a triangular distribution of horizontal forces is used, whereas in case of base isolated buildings an orthogonal distribution is adopted. The position of the OTA is defined by the coordinates x_T and y_T of its intersection point with the Oxy plane.

$$x_T = \frac{-\boldsymbol{\theta}_{z,y}^T \boldsymbol{\theta}_{z,z}}{\boldsymbol{\theta}_{z,z}^T \boldsymbol{\theta}_{z,z}} \tag{5}$$

$$y_T = \frac{\boldsymbol{\theta}_{z,x}^T \boldsymbol{\theta}_{z,z}}{\boldsymbol{\theta}_{z,z}^T \boldsymbol{\theta}_{z,z}} \tag{6}$$

where

$\boldsymbol{\theta}_{z,x}$ are the rotations due to the action of forces $\mathbf{F}_x$, with $\mathbf{F}_x = 1 \cdot \mathbf{F}$ the vector of the forces $\mathbf{F}$ when acting parallel to the axis Ox.

$\boldsymbol{\theta}_{z,y}$ are the rotations due to the action of forces $\mathbf{F}_y$, with $\mathbf{F}_y = 1 \cdot \mathbf{F}$ the vector of the forces $\mathbf{F}$ when acting parallel to the axis Oy.

$\boldsymbol{\theta}_{z,z}$ are the rotations due to the action of moments $\mathbf{M}_z$, with $\mathbf{M}_z = 1 \cdot \mathbf{F}$ the vector of the torsional moments $\mathbf{M}$ about axis Oz which have the same distribution with the horizontal forces $\mathbf{F}$.

Based on the above procedure, the OTA for the fully fixed to the ground buildings (case (a)), as well as for the buildings resting on the isolators without eccentricity (case (b)), was determined (figure 2). Moreover, as mentioned before, in case (c), the isolators' effective stiffness was chosen so as the optimum torsion axis of the structure to coincide with the vertical mass axis. In order to fulfill the above criterion the distribution of the isolators' horizontal effective stiffness given in figure 3 is considered.

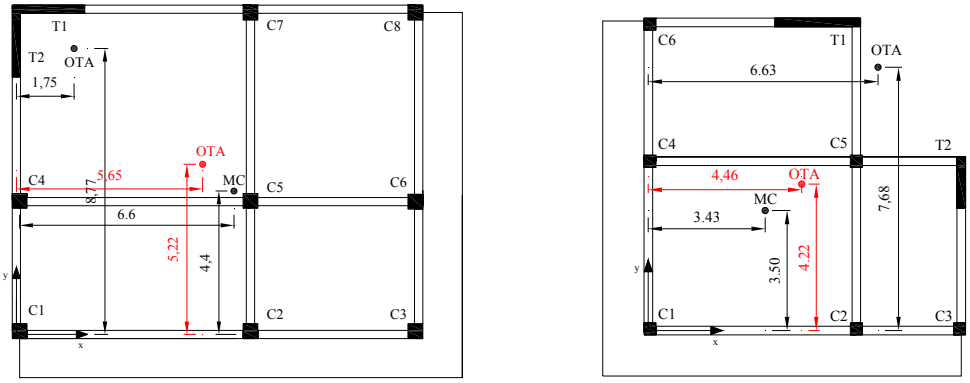

(a) (b)

Figure 2. Location of the OTA for the fully fixed to the ground buildings and for the buildings resting on the isolators without eccentricity (red color). Building B1 (a) and B2 (b) (MC: Mass Centre)

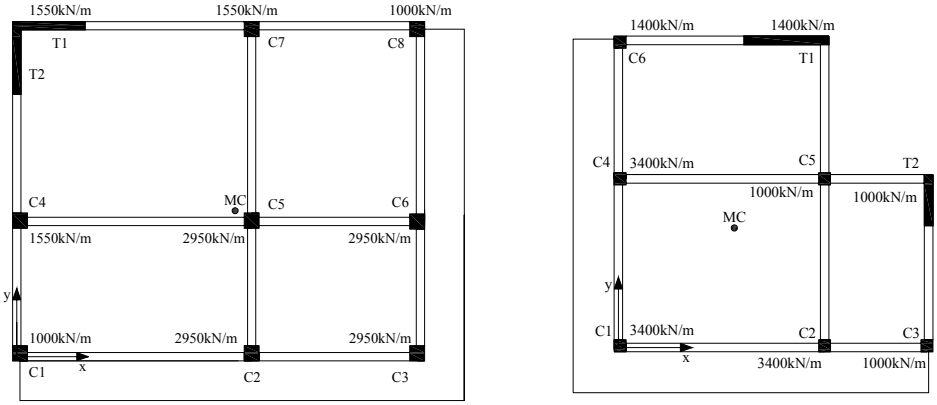

(a) (b)

Figure 3. Distribution of the isolators' horizontal effective stiffness for model (c) (building B1 (a) and building B2 (b))

3 LINEAR TIME HISTORY ANALYSES

The influence of the two different distributions of isolators' effective stiffness on the linear response of the two buildings considered in the present study (B1 and B2) was evaluated by means of linear analyses. More specifically, linear time history analyses under three bidirectional seismic strong motions (recorded during El Centro, Kobe and Lefkada earthquakes) were performed and the maximum response over all seismic incident angles was determined with the aid of analytical formulae [13]. For each building two different models were considered accounting for the cases (b) and (c) of isolators. The analyses were performed with the aid of the computer program SAP2000 [14]. The base isolators were

modeled using NLink elements of the rubber isolator type. The hysteretic model used to simulate the inelastic behavior of the base isolators along two orthogonal horizontal axes is shown in figure 4. The post-yield stiffness k_2 was taken equal to $0.1k_1$, where k_1 is the elastic stiffness. The yield force V_y was taken equal to 10% of the total weight of the structure.

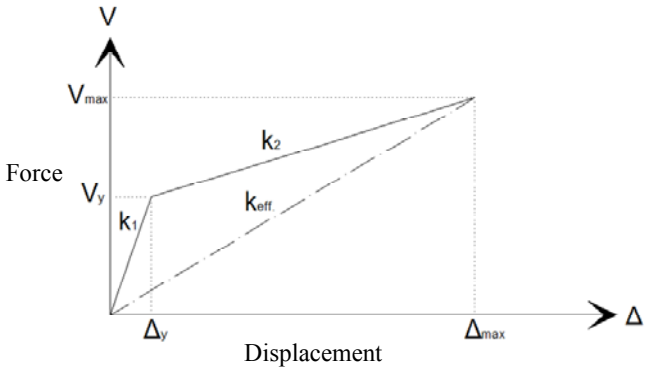

Figure 4. Hysteretic model for the base isolators.

3.1 Critical orientation and maximum response

General

The structure is subjected to bidirectional horizontal seismic motion consisting of the accelerograms $\ddot{u}_{ag}(t)$ and $\ddot{u}_{bg}(t)$. As the direction of the seismic motion is unknown, they can form any angle θ with the x and y structural axes (figure 5a). We consider two orientations of the seismic excitation:

(i) Excitation ‘α0’: The accelerograms $\ddot{u}_{ag}(t)$ and $\ddot{u}_{bg}(t)$ are applied along the axes x and y, respectively, i.e. the angle of seismic incidence is $\theta=0^o$ (figure 5b). A typical response quantity R is denoted as $R_{,\alpha 0}$.

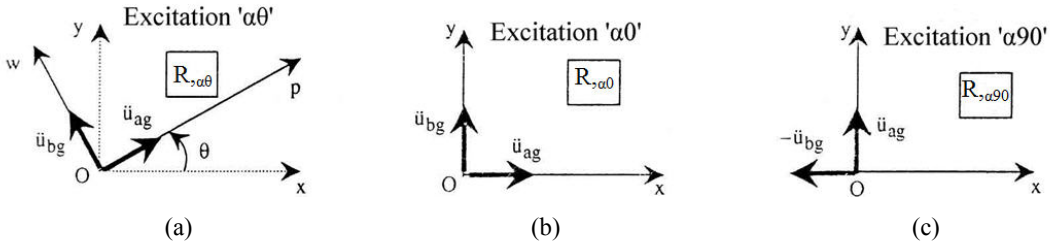

Figure 5. Excitations ‘αθ’ (a), ‘α0’ (b) and ‘α90’ (c)

(ii) Excitation ‘α90’: The accelerograms $\ddot{u}_{ag}(t)$ and $\ddot{u}_{bg}(t)$ are applied along the axes y and x, respectively, i.e. the angle of seismic incidence is $\theta=90^o$ (figure 5c). A typical response quantity R is denoted as $R_{,\alpha 90}$.

It has been proved [13] that the maximum value of a response parameter for any angle θ of seismic incidence is given, as a function of time, by the relation:

$$R_o(t) = \left(R^2_{,\alpha 0}(t) + R^2_{,\alpha 90}(t) \right)^{1/2} \tag{7}$$

The plot of the function $\pm R_0(t)$ provides the maximum/minimum value of the required response parameter as well as the time instant t_{cr} at which the maximum/minimum occurs.

$$\max R = +R_0(t_{cr}) \quad \text{and} \quad \min R = -R_0(t_{cr}) \tag{8}$$

The corresponding critical angles θ_{cr1} (maximum value) and θ_{cr2} (minimum value) are given by the relations [13]:

$$\theta_{cr1} = \tan^{-1}\left(\frac{R_{,\alpha 90}(t_{cr})}{R_{,\alpha 0}(t_{cr})}\right) \text{ and } \theta_{cr2} = \theta_{cr1} - \pi \tag{9}$$

Displacement vector

The horizontal displacements at any point of the building's floors are usually computed along the (ξ, η) axes of an appropriate local reference system. The displacement vector u is related to u_ξ and u_η through the relation: $u^2(t) = u_\xi^2(t) + u_\eta^2(t)$ (figure 6). Subscripts ξ and η characterize the axis along which the displacement is computed.

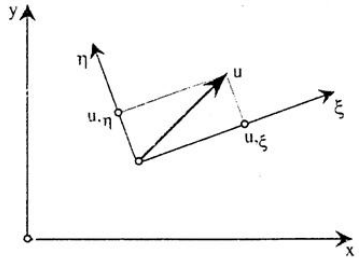

Figure 6. Displacement vector u

Thus, the response quantities $u_{,\alpha 0}^2(t)$ and $u_{,\alpha 90}^2(t)$ are given by the following relations:

$$u_{,\alpha 0}^2(t) = u_{\xi,\alpha 0}^2(t) + u_{\eta,\alpha 0}^2(t) \tag{10}$$

$$u_{,\alpha 90}^2(t) = u_{\xi,\alpha 90}^2(t) + u_{\eta,\alpha 90}^2(t) \tag{11}$$

The meanings of the subscripts remain the same as in the previous paragraph. The parameter u_{xy} is defined as:

$$u_{xy}(t) = u_{\xi,\alpha 0}(t) \cdot u_{\xi,\alpha 90}(t) + u_{\eta,\alpha 0}(t) \cdot u_{\eta,\alpha 90}(t) \tag{12}$$

The plot of the function $u_{,I}(t)$ (equation 13) provides all the information necessary to compute the maximum value of the displacement u_{cr} and the associated time instant t_{cr} [13]:

$$u_{cr}^2 = \max u_{,I}^2(t) = u_I^2(t_{cr}) = \frac{u_{,\alpha 0}^2(t_{cr}) + u_{,\alpha 90}^2(t_{cr})}{2} + \sqrt{\left(\frac{u_{,\alpha 0}^2(t_{cr}) - u_{,\alpha 90}^2(t_{cr})}{2}\right)^2 + u_{xy}^2(t_{cr})} \tag{13}$$

The corresponding critical angle θ_{cr} is determined by the angle θ_o (equation 14) with the aid of figure 7 [13]:

$$\theta_o = \frac{1}{2}\tan^{-1}\left(\frac{2u_{xy}(t_{cr})}{u_{,\alpha 0}^2(t_{cr}) - u_{,\alpha 90}^2(t_{cr})}\right) \tag{14}$$

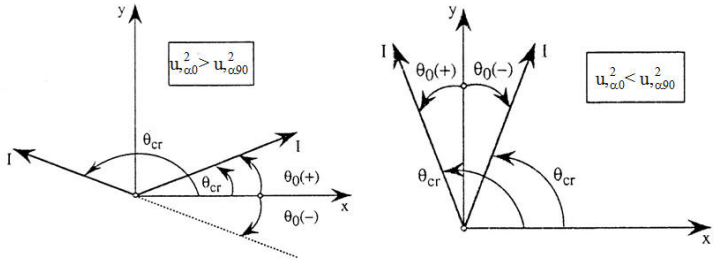

Figure 7. Determination of critical angle θ_o

3.2 Analyses results

Tables 3 and 4 present the displacements $u_{,I}^2$ (see section 3.1) as well as the associated critical time instant t_{cr} and critical incident angle θ_{cr} of the vertical structural elements at the level of the isolators (Table 3) and of the 3rd floor (Table 4). The tables regard the building B1 subjected to the earthquake record of El Centro. Moreover, in table 5 the maximum values of the floor rotations over all incident angles R_z, as well as the floor rotations due to excitations α0 and α90 (see section 3.1) are presented. From these tables we can see that for the same earthquake record different response quantities have different critical incident angles. Furthermore, note that the same response quantities have different critical incident angles for the two cases of isolators, since, as it can be seen from the tables, the critical incident angle of a certain response quantity depends on the distribution of the isolators' stiffness.

	Isolators without eccentricity			**Isolators with eccentricity**		
	$\mathbf{u_{,I}^2}$	$\mathbf{t_{cr}}$	$\boldsymbol{\theta_{cr}}$	$\mathbf{u_{,I}^2}$	$\mathbf{t_{cr}}$	$\boldsymbol{\theta_{cr}}$
C1	0.00481	12.30	79.34	0.00282	2.94	106.48
C2	0.00427	2.30	52.73	0.00264	2.95	2.94
C3	0.00583	2.96	74.10	0.00264	2.95	13.92
C4	0.00371	12.30	65.91	0.00285	2.94	90.80
C5	0.00314	2.95	75.23	0.00301	2.95	32.24
C6	0.00466	2.95	90.36	0.00268	2.95	31.87
C7	0.00310	2.93	134.36	0.00282	2.95	58.83
C8	0.00455	2.94	111.36	0.00277	2.95	45.89
T1	0.00279	12.30	43.79	0.00292	2.95	75.22
T2	0.00308	12.30	49.89	0.00292	2.95	79.29

Table 3: Displacements $u_{,I}^2$ of the vertical structural elements (basement) and critical incident angles in case of building B1 subjected to earthquake record of El Centro

	Isolators without eccentricity			Isolators with eccentricity		
	$u_{,I}^2$	t_{cr}	θ_{cr}	$u_{,I}^2$	t_{cr}	θ_{cr}
C1	0.00765	12.30	89.32	0.00467	2.96	17.99
C2	0.00717	2.98	54.88	0.00471	2.96	56.77
C3	0.00997	2.97	76.09	0.00496	2.96	79.75
C4	0.00578	12.31	71.73	0.00455	2.95	179.49
C5	0.00489	2.95	23.25	0.00478	2.96	56.23
C6	0.00806	2.96	92.75	0.00482	2.96	97.82
C7	0.00541	2.94	134.87	0.00460	2.95	136.17
C8	0.00794	2.95	112.45	0.00479	2.95	119.18
T1	0.00452	2.95	71.39	0.00451	2.95	157.32
T2	0.00470	12.30	51.14	0.00451	2.95	162.52

Table 4: Displacements $u_{,I}^2$ of the vertical structural elements (3rd floor) and critical incident angles in case of building B1 subjected to earthquake record of El Centro

	Isolators without eccentricity				
	$R_{z,\alpha 0}$	$R_{z,\alpha 90}$	R_z	t_{cr}	θ_{cr}
Basement	-1.240E-03	-3.670E-03	3.874E-03	2.97	71.33
1st storey	-1.350E-03	-4.060E-03	4.279E-03	2.96	71.61
2nd storey	-1.450E-03	-4.460E-03	4.690E-03	2.96	71.99
3rd storey	-1.530E-03	-4.870E-03	5.105E-03	2.96	72.56

	Isolators with eccentricity				
	$R_{z,\alpha 0}$	$R_{z,\alpha 90}$	R_z	t_{cr}	θ_{cr}
Basement	-1.700E-04	-4.510E-04	4.817E-04	2.33	69.33
1st storey	-1.280E-04	-2.640E-04	2.931E-04	2.33	64.08
2nd storey	-1.720E-04	-2.390E-04	2.946E-04	3.02	54.32
3rd storey	-2.540E-04	-5.360E-04	5.931E-04	3.03	64.68

Table 5: Floor rotations R_z and critical incident angles in case of building B1 subjected to earthquake record of El Centro

In order to better illustrate the differences between the two cases of isolators, figures 8-15 present the displacements $u_{,I}^2$ of the vertical structural elements, as well as the maximum floor rotations R_z, computed with the aid of the methodology proposed in [13] (see section 3.1), for the three earthquake records considered. Figures 8-11 correspond to the building B1, whereas figures 12-15 correspond to the building B2.

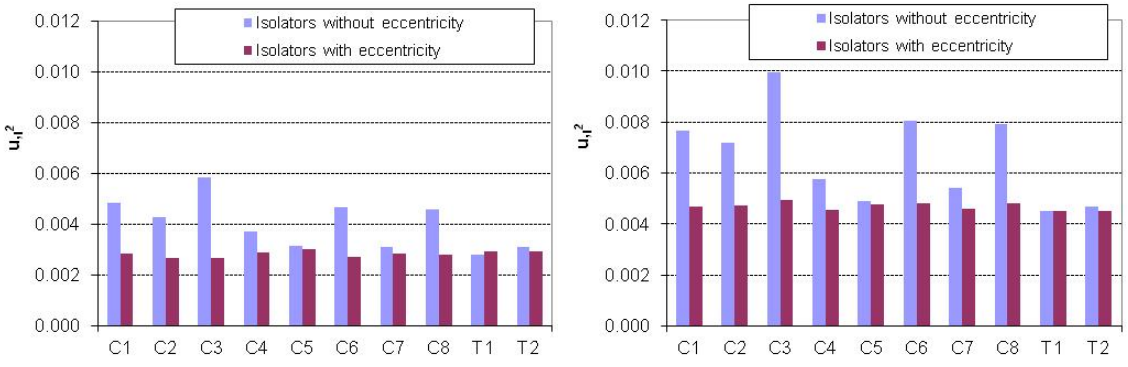

(a) (b)

Figure 8: Displacements $u_{,I}^2$ of the vertical structural elements (basement (a) and 3rd floor (b)) in case of building B1 subjected to earthquake record of El Centro

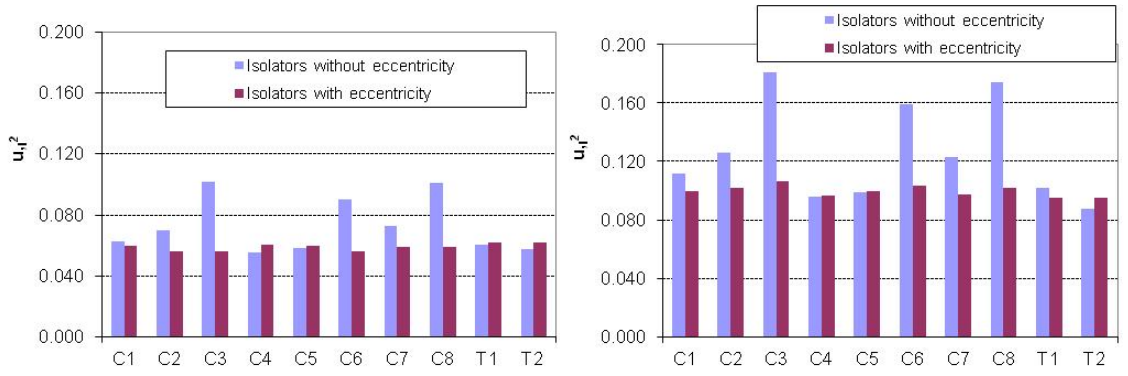

(a) (b)

Figure 9: Displacements $u_{,I}^2$ of the vertical structural elements (basement (a) and 3rd floor (b)) in case of building B1 subjected to earthquake record of Kobe

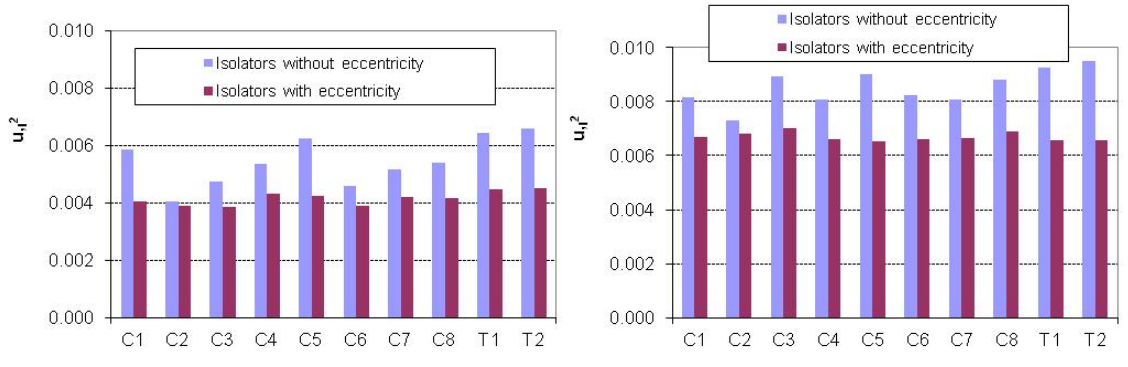

(a) (b)

Figure 10: Displacements $u_{,I}^2$ of the vertical structural elements (basement (a) and 3rd floor (b)) in case of building B1 subjected to earthquake record of Lefkada

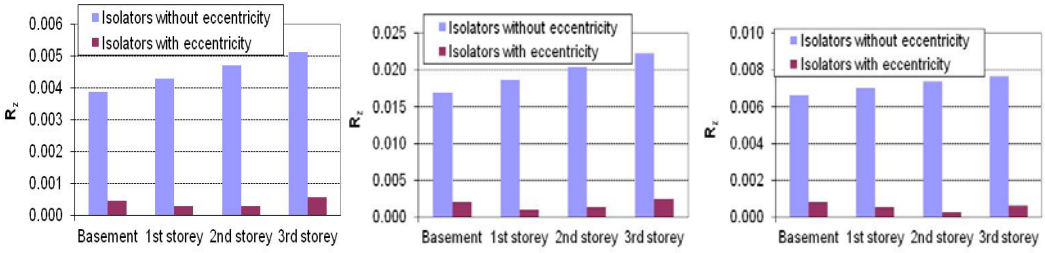

(a) (b) (c)

Figure 11: Floor rotations R_z in case of building B1 subjected to earthquake records of El Centro (a), Kobe (b) and Lefkada (c)

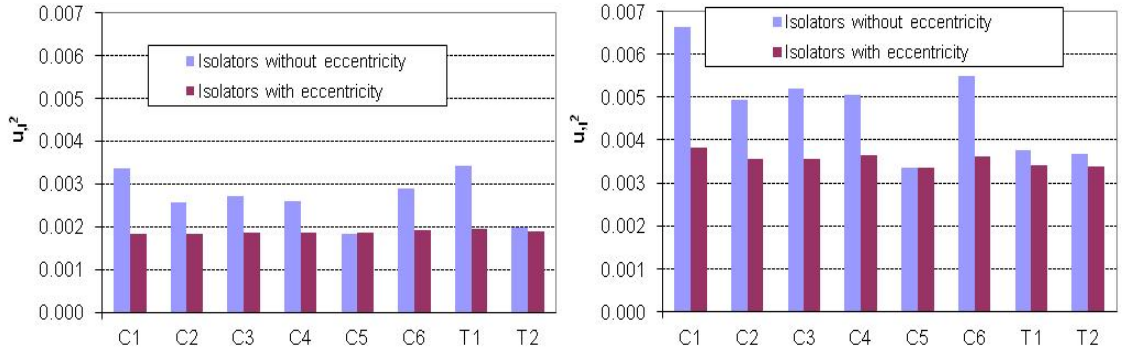

(a) (b)

Figure 12: Displacements $u_{,I}^2$ of the vertical structural elements (basement (a) and 3rd floor (b)) in case of building B2 subjected to earthquake record of El Centro

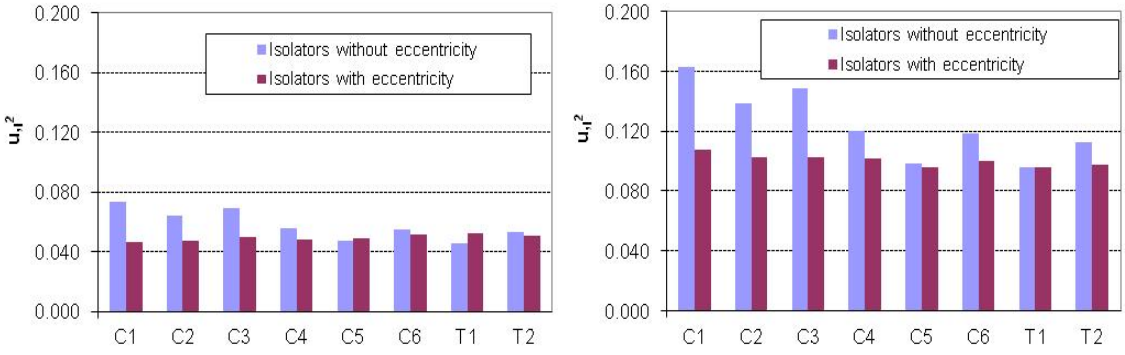

(a) (b)

Figure 13: Displacements $u_{,I}^2$ of the vertical structural elements (basement (a) and 3rd floor (b)) in case of building B2 subjected to earthquake record of Kobe

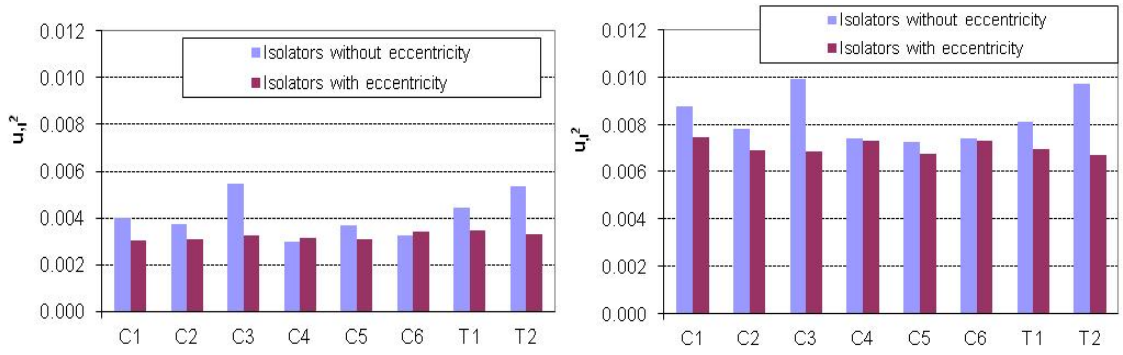

(a) (b)

Figure 14: Displacements $u_{,I}^2$ of the vertical structural elements (basement (a) and 3rd floor (b)) in case of building B2 subjected to earthquake record of Lefkada

(a) (b) (c)

Figure 15: Floor rotations R_z in case of building B2 subjected to earthquake records of El Centro (a), Kobe (b) and Lefkada (c)

We can see that the displacements of the vertical structural elements in most cases are smaller when the buildings rest on the isolators with eccentricity. Note that the displacements can be up to 55% smaller (column C3 at the level of the isolators) for the building B1 (figure 8a) and up to 46% smaller (column C1 at the level of the isolators) for the building B2 (figure 12a). The reduction of the displacements that is achieved in case of the isolators with eccentricity is larger for the structural elements of the flexible side of the buildings. However, the displacements of the structural elements located at the stiff side can be either reduced or increased depending on the earthquake record. The above conclusion is valid for both the buildings investigated in the present study. For example, note that the displacement of the wall T2 (building B1) is smaller for the isolators with eccentricity in case of the earthquake records of El Centro and Lefkada (figures 8 and 10). The opposite observation can be made when the building is subjected to the earthquake record of Kobe (figure 9). Of great significance is also the fact that when isolators with eccentricity are used the analyses produce displacements which have almost the same value for all the vertical structural elements. With regard to the floor rotations, figures 11 and 15 show that they are much smaller in case of the isolators with eccentricity (up to 25 times smaller for building B1 (figure 11c) and up to 20 times smaller for building B2 (figure 15b).

4 NONLINEAR TIME HISTORY ANALYSES

In order to evaluate the influence of the two different distributions of isolators' effective stiffness on the nonlinear response, the two buildings considered in the present study (B1 and

B2) were analyzed by Nonlinear Time History Analysis (NTHA) for each one of the three earthquake ground motions presented in the previous section. For each building two different models were considered accounting for the distributions (b) and (c) of isolators properties. The analyses were performed with the aid of the computer program SAP2000 [14] and assuming the inelasticity concentrated on the isolators while the superstructure behaves elastically. Furthermore, in order to determine the maximum response over all incident angles, the two horizontal accelerograms of each ground motion were applied along horizontal orthogonal axes forming with the structural axes an angle θ=0°, 30°, 60°, …, 150°. Thus, for each building and each pair of accelerograms six orientations were considered. As a consequence a total of 72 NTHA (2 buildings x 2 cases of isolators x 3 earthquake records x 6 incident angles) were conducted in the present study. For each ground motion and incident angle, the damage state of the two buildings was determined. The seismic response was expressed in terms of the displacements of the vertical structural elements at the level of the isolation (basement), as well as of the floor rotations.

Table 6 presents the maximum displacements of the vertical structural elements over all incident angles at the level of the isolators (basement) and the associated critical time instant and critical incident angle. We can see that the displacements of all the vertical elements are approximately equal when isolators with eccentricity are used.

Figure 16 (building B1) and figure 18 (building B2) present the maximum displacements of the vertical structural elements for the three earthquake records considered. Figure 17 (building B1) and figure 19 (building B2) present the maximum floor rotations for the three earthquake records considered.

	Isolators without eccentricity			**Isolators with eccentricity**		
	maxu	**t_{cr}**	**θ_{cr}**	**maxu**	**t_{cr}**	**θ_{cr}**
C1	0.10996	4.49	0	0.10089	8.80	90
C2	0.14330	2.98	30	0.09913	4.48	120
C3	0.12006	4.51	30	0.09886	4.48	150
C4	0.10425	4.48	150	0.10067	8.80	90
C5	0.10023	4.48	120	0.10023	4.48	90
C6	0.11217	4.51	60	0.09873	4.49	150
C7	0.10282	4.49	120	0.09964	4.48	30
C8	0.11232	4.50	90	0.09933	4.49	0
T1	0.09909	4.48	120	0.10105	4.48	60
T2	0.09962	4.48	150	0.10131	4.48	0

Table 6: Maximum displacements of the vertical structural elements (basement) and critical incident angles in case of building B1 subjected to earthquake record of El Centro

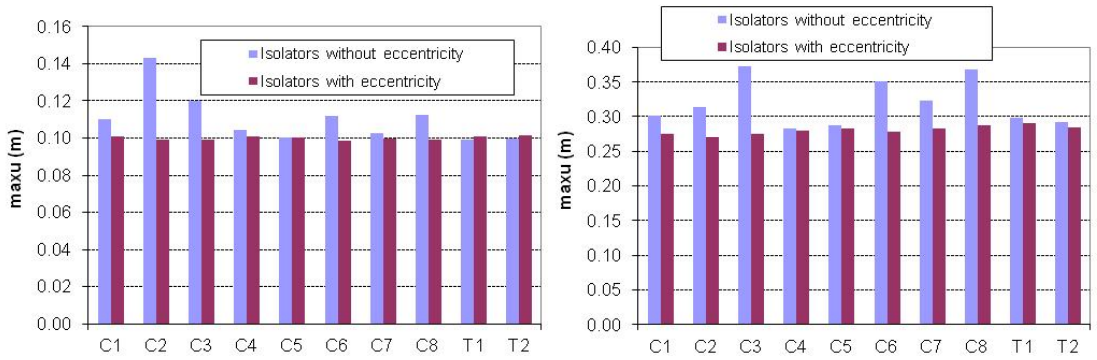

(a)

(b)

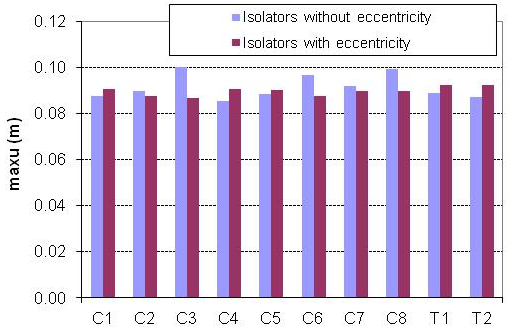

(c)

Figure 16: Maximum displacements of the vertical structural elements (basement) in case of building B1 subjected to earthquake records of El Centro (a), Kobe (b) and Lefkada (c)

It can be seen that the displacements of the vertical structural elements located at the flexible side of the building are smaller [up to 45% for the column C2 of the building B1 (figure 16a) and up to 38% smaller for the column C1 of the building B2 (figure 18a)] when the buildings rest on the isolators with eccentricity. Concerning the displacements of the structural elements located at the stiff side, note that they can be either reduced or increased depending on the earthquake record. For example, we can see that the displacement of the column C4 (building B1) is smaller in the case of the isolators with eccentricity for the earthquake record of El Centro (figure 16a). However, when the same building is subjected to the earthquake record of Lefkada, the displacement of the column C4 is smaller in case of the isolators without eccentricity (figure 16c). As it was mentioned in the case of the linear analyses, the displacements produced when isolators with eccentricity are used have almost the same value for all the vertical structural elements. Finally, figures 17 and 19 show that the floor rotations are much smaller in case of the isolators with eccentricity (up to 16 times smaller for building B1 (figure 17c) and up to 8 times smaller for building B2 (figure 19a). The difference between the values of the displacements produced for the two different distributions of isolators' stiffness depends on the earthquake record. See for example that seismic motion of Kobe led to smaller differences among the floor rotations compared to the differences produced when the seismic records of El Centro or Lefkada were used for the analyses.

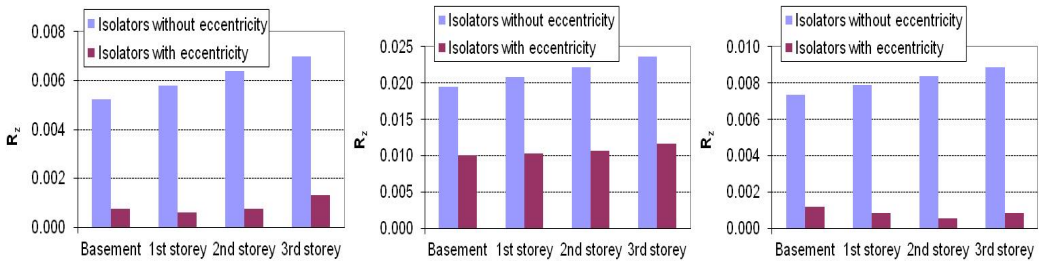

(a) (b) (c)

Figure 17: Maximum floor rotations in case of building B1 subjected to earthquake records of El Centro (a), Kobe (b) and Lefkada (c)

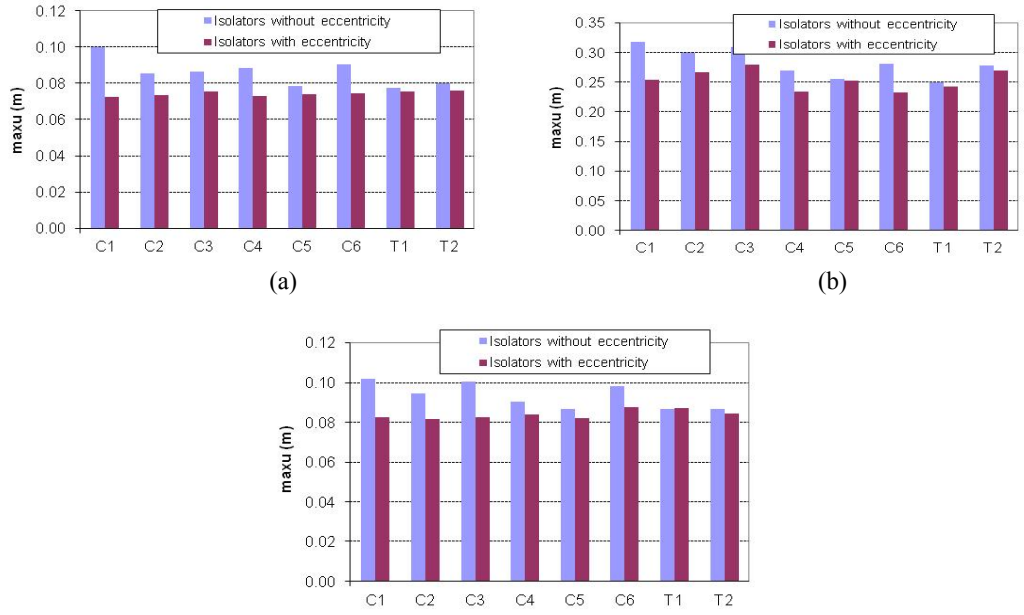

(a) (b)

(c)

Figure 18: Maximum displacements of the vertical structural elements (basement) in case of building B2 subjected to earthquake records of El Centro (a), Kobe (b) and Lefkada (c)

(a) (b) (c)

Figure 19: Maximum floor rotations in case of building B2 subjected to earthquake records of El Centro (a), Kobe (b) and Lefkada (c)

5 CONCLUSIONS

The present study examines the influence of the isolators' effective stiffness distribution on the torsional response of base isolated structures. To accomplish this purpose two R/C 3-storey buildings were analyzed under earthquake ground motions for the following two distributions of isolators' effective stiffness: (a) all the isolators have identical horizontal stiffness and (b) the isolators' effective stiffness is chosen so as the optimum torsion axis of the structure to coincide with the vertical mass axis. The two buildings were subjected to linear as well as nonlinear time history analyses under three bidirectional earthquake ground motions. For each earthquake record the maximum response over all incident angles of seismic motion was determined. Based on the analyses results of the study, the following conclusion can be drawn:

- When the isolators' effective stiffness is chosen so as the optimum torsion axis of the structure to coincide with the vertical mass axis (isolators with eccentricity) the analysis produces displacements which have almost the same value for all the vertical structural elements.
- The displacements of the vertical structural elements located at the flexible side of the buildings are smaller in case of the isolators with eccentricity compared to the corresponding ones produced when all the isolators possess the same stiffness. However, the displacements of the structural elements located at the stiff side can be either reduced or increased depending on the earthquake record.
- The floor rotations are much smaller in case of the isolators with eccentricity. The difference between the values of the floor rotations produced for the two different distributions of isolators' stiffness depends on the earthquake record.

It must be noted that the aforementioned conclusions are valid for the buildings and ground motions used in the present study. In order to expand them to other structural systems, further investigation is necessary.

6 ACKNOWLEDGEMENTS

This study was financially supported by "IKY FELLOWSHIPS OF EXCELLENCE FOR POSTGRADUATE STUDIES IN GREECE - SIEMENS PROGRAM".

REFERENCES

[1] R.L. Crosbie, *Base isolation for brick masonry shear wall structures*, MEng Thesis, University of Canterbury, Christchurch, NZ, 1977.

[2] D.M. Lee, Base isolation for torsion reduction in asymmetric structures under earthquake loadings, *Earthquake Engineering and Structural Dynamics,* **8(4)**, 349-359, 1980.

[3] A. Tena-Colunga, J.L. Escamilla-Cruz, Torsional amplifications in asymmetric base-isolated structures, *Engineering Structures*, **29(2)**, 237-247, 2007.

[4] V. Kilar, D. Koren, Seismic behaviour of asymmetric base isolated structures with various distributions of isolators", *Engineering structures*, **31(4)**, 910-921, 2009.

[5] Eurocode 2 (2004) Design of concrete structures, Part 1-1: General rules and rules for buildings, European Committee for Standardization, Brussels, Belgium, 2004.

[6] Eurocode 8 (1998-1), Design provisions for earthquake resistance of structures, European Committee for Standardization, Brussels, Belgium, 2003.

[7] C.E. Seguin, J.L. Almazán, J.C. De la Llera, Torsional balance of seismically isolated asymmetric structures, *Engineering structures*, **46**, 703-717, 2013.

[8] FEMA 356. Prestandard and commentary for the seismic rehabilitation of buildings, Federal Emergency Management Agency, Washington, DC, 2000.

[9] ASCE 41/06. Seismic Rehabilitation of Existing Buildings, American Society of Civil Engineers, 2009.

[10] http://www.bridgestone.com/products/diversified/antiseismic_rubber/principle.html

[11] E.M. Marino, P.P. Rossi, Exact evaluation of the location of the optimum torsion axis. *Structural Design of Tall and Special Buildings*, **13(4)**, 277-290, 2004.

[12] J.N. Doudoumis, A.M. Athanatopoulou, Invariant torsion properties of multistorey asymmetric buildings. *Structural Design of tall and Special Buildings*, **17(1)**, 79-97, 2008.

[13] A.M. Athanatopoulou, Critical orientation of three correlated seismic components. *Engineering Structures*, **27(2)**, 301-312, 2005.

[14] SAP2000, Computers and Structures Inc, CSI, Berkeley.